

## Analysis of the magnetic properties of $R_2\text{Co}_{17}$ ( $R = \text{Pr, Nd, Sm, Gd, Tb, Dy, Ho, and Er}$ )

Han Xiu-feng, Jin Han-min, Wang Zi-jun, and T. S. Zhao

*Department of Physics, Jilin University, Changchun 130023, People's Republic of China*

C. C. Sun

*Institute of Theoretical Chemistry, Jilin University, Changchun 130023, People's Republic of China*

(Received 5 May 1992; revised manuscript received 5 October 1992)

High-field isotherms at low and high temperatures and other magnetic properties of  $R_2\text{Co}_{17}$  ( $R = \text{Pr, Nd, Sm, Gd, Tb, Dy, Ho, and Er}$ ) measured on single crystals are analyzed on the basis of the single-ion model. The fitted crystalline electric-field parameter  $A_{20}$  for the Pr ion is several times smaller in absolute value than those for all the other rare-earth ions. The result is similar to that observed in the  $R\text{Co}_5$  series, and it is suggested that the Pr ion in  $\text{Pr}_2\text{Co}_{17}$ , as in  $\text{PrCo}_5$ , is valence fluctuated.

### I. INTRODUCTION

For most  $R_2\text{Co}_{17}$  ( $R = \text{rare earth}$ ) compounds, the high-field isotherms of single crystals along the principal crystal axes and other magnetic properties have been studied in a number of papers, and the isotherms at 4.2 K have been analyzed within a classical two-sublattice model.<sup>1-10</sup> The isotherms and the energy-level scheme, all at 4.2 K, have also been analyzed for  $\text{Ho}_2\text{Co}_{17}$  in terms of crystal- and molecular-field interaction.<sup>11</sup>

It is our experience, however, that in many cases the low-temperature isotherms, by themselves, do not provide sufficient information about the crystalline electric-field (CEF) parameters. The aim of the present work is to evaluate the values of the exchange and CEF parameters from the experimental data of the isotherms at low and high temperatures, as well as some other magnetic prop-

erties for a series of  $R_2\text{Co}_{17}$  ( $R = \text{Pr, Nd, Sm, Gd, Tb, Dy, Ho, and Er}$ ), using the single-ion model, and to analyze the experimental data.

### II. METHOD OF ANALYSIS

$R_2\text{Co}_{17}$  has  $\text{Th}_2\text{Zn}_{17}$ -type rhombohedral structure with space group  $R\bar{3}m$  for  $R = \text{Y, Pr, Nd, Sm, and Gd}$ , and  $\text{Th}_2\text{Ni}_{17}$ -type hexagonal structure with space group  $P6_3/mmc$  for  $R = \text{Tb, Dy, Ho, and Er}$ . There is one rare-earth crystallographic site in the rhombohedral structure, and two sites,  $b$  and  $d$ , in the hexagonal structure. Each site splits into two magnetically nonequivalent sites  $A$  and  $B$ . In the coordinate system with the  $z$  and  $x$  axes along the  $c$  and  $a$  axes, the Hamiltonian of the CEF interaction for the rare-earth ions at the  $A$  and  $B$  sites are closely related, being represented as

TABLE I. The fitted values of  $2\mu_B H_{\text{ex}}(0)$ ,  $A_{nm}$ ,  $K_{1\text{Co}}(0)$ , and  $M_{\text{Co}}(0)$ , and the values of  $M_R(0)$ , calculated by using the parameters for  $R_2\text{Co}_{17}$ .

$R$	$2\mu_B H_{\text{ex}}(0)$ (K)	$A_{20}$ (K)	$A_{40}$ (K)	$A_{60}$ (K)	$A_{66}$ (K)	$K_{1\text{Co}}(0)$ (K/f.u.)	$M_{\text{Co}}(0)$ ( $\mu_B$ /f.u.)	$M_R(0)$ ( $\mu_B/R$ )
Pr	600	-80	-260	10	-300	-8.0	27.7	3.10
Nd	500	-250	-270	30	-350	-8.0	27.6	3.13
Sm	350	-220	0	0	-300	-8.0	26.9	0.40
Gd	260					-8.0	27.7	7.00
Tb	250	-200	-100	50	-130	-9.0	27.9	8.99
Dy	230	-220	-230	50	-120	-9.0	27.4	10.0
Ho	210	-200	-150	50	-110	-9.0	27.7	9.93
Er	210	-260	-130	50	-100	-9.0	29.6	9.00
Tm <sup>a</sup>	200	-200	-120	50	-100	-9.0	27.6	7.00
Ho( $b$ )	213	-522	-144	167	-112	-7.05	28.01	(Ref. 11)
Ho( $d$ )	213	-180	197	224	-112	-7.05	28.01	(Ref. 11)
Ho(average)	213	-351	26	196	-112	-7.05	28.01	(Ref. 11)

<sup>a</sup>The values of the  $A_{40}$ ,  $A_{60}$ ,  $A_{66}$  and  $K_{1\text{Co}}(0)$  are estimated from the extrapolation of those for the other rare earths.

$$\begin{aligned} \mathcal{H}_{\text{CEF}}(A) &= \sum_{n=2,4,6} A_{n0} C_{n0} + \sum_{n=4,6} A_{n3} (C_{n3} + C_{n-3}) \\ &\quad + A_{66} (C_{66} + C_{6-6}), \\ \mathcal{H}_{\text{CEF}}(B) &= \sum_{n=2,4,6} A_{n0} C_{n0} - \sum_{n=4,6} A_{n3} (C_{n3} + C_{n-3}) \\ &\quad + A_{66} (C_{66} + C_{6-6}), \end{aligned} \quad (1)$$

where

$$C_{nn} = \sum_j [4\pi/(2n+1)]^{1/2} Y_{nm}(\theta_j, \varphi_j). \quad (2)$$

$Y_{nm}(\theta_j, \varphi_j)$  are the spherical harmonics, and  $\theta_j$  and  $\varphi_j$  are the polar and azimuthal angles of the position vector of the  $j$ th  $4f$  electron. The sign of the second term in the right of Eq. (1) is opposite for  $\mathcal{H}_{\text{CEF}}(A)$  and  $\mathcal{H}_{\text{CEF}}(B)$ , and the contributions of each of them, to the total energy of the compound, largely cancel each other.

Neglecting the second terms, the Hamiltonian of the

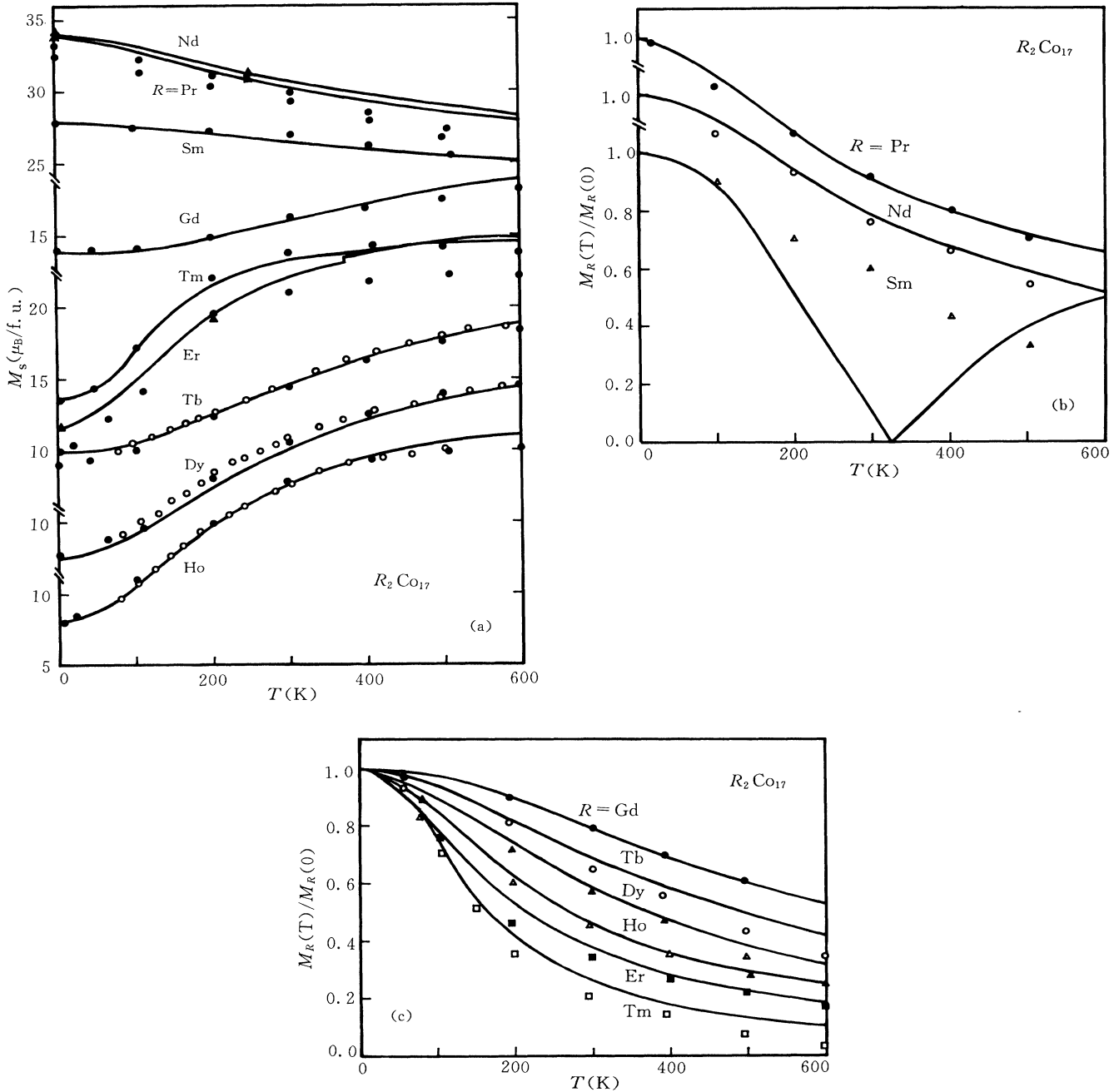


FIG. 1. Temperature dependence of spontaneous magnetizations (a) and the normalized magnetic moments for the rare-earth ions (b), (c) for the  $R_2Co_{17}$  series. The solid lines represent the calculations. The experimental data ( $\circ$ ), ( $\bullet$ ), and ( $\blacktriangle$ ) are taken from (a) Refs. 1, 2, and 3, respectively and ( $\bullet$ ) etc. from (b), (c) Ref. 2.

CEF interaction, averaged over the crystallographic and magnetic nonequivalent sites, therefore, is expressed simply as

$$\mathcal{H}_{\text{CEF}} = \sum_{n=2,4,6} A_n C_{n0} + A_{66}(C_{66} + C_{6-6}). \quad (3)$$

The total Hamiltonian of the rare-earth ion consists of the spin-orbit interaction, the CEF interaction, the R-Co exchange interaction, and the Zeeman energy, that is,

$$\mathcal{H}_R = \lambda \mathbf{L} \cdot \mathbf{S} + \mathcal{H}_{\text{CEF}} + 2\mu_B \mathbf{S} \cdot \mathbf{H}_{\text{ex}} + \mu_B [\mathbf{L} + 2\mathbf{S}] \cdot \mathbf{H}. \quad (4)$$

The R-R exchange interaction, which is much weaker than the R-Co exchange interaction, is neglected.

$\mathbf{H}_{\text{ex}}(T)$  is assumed to be proportional and antiparallel to the magnetic moment of the Co sublattice  $\mathbf{M}_{\text{Co}}(T)$ . The matrix elements of Eq. (4) are calculated by using the irreducible-tensor-operator technique.<sup>12</sup> For a given applied field  $\mathbf{H}$  and a direction of  $\mathbf{H}_{\text{ex}}$ , the eigenvalues  $E_i$  and eigenfunctions  $|n_i\rangle [i=1,2,\dots,\sum_J(2J+1)]$  are obtained by diagonalizing the  $\sum_J(2J+1) \times \sum_J(2J+1)$  matrix of Eq. (4). The diagonalization was carried out within the subspace consisting of the ground and the first excited  $J$  multiplets for the Pr and Nd ions with  $\lambda=610$  and 536 K, respectively,<sup>13</sup> within the subspace consisting of the ground and the two lowest excited  $J$  multiplets for the Sm ion with  $\lambda=410$  K,<sup>13</sup> and within the subspace of the ground  $J$  multiplet for the heavy rare-earth ions. The free energy for  $R_2\text{Co}_{17}$  is given by

$$F(\mathbf{H}, \mathbf{H}_{\text{ex}}, T) = -2k_B T \ln Z + K_{1\text{Co}}(T) \sin^2 \theta_{\text{Co}} - \mathbf{M}_{\text{Co}}(T) \cdot \mathbf{H}, \quad (5)$$

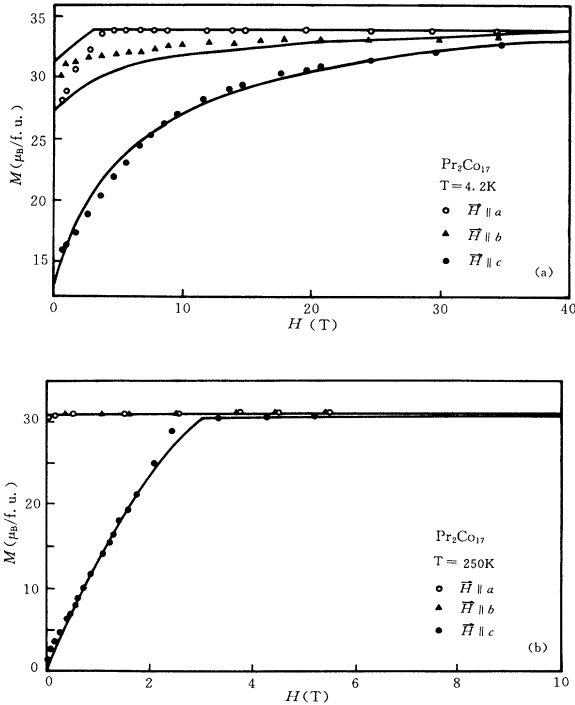


FIG. 2. Isotherms at (a) 4.2 K and (b) 250 K for  $\text{Pr}_2\text{Co}_{17}$ . The solid lines represent the calculations. The experimental data ( $\circ$ ,  $\blacktriangle$ ,  $\bullet$ ) are from Ref. 4.

where

$$Z = \sum_i \exp(-E_i/k_B T), \quad (6)$$

and  $K_{1\text{Co}}$  is the magnetocrystalline anisotropy constant of the Co sublattice.  $M_{\text{Co}}(T/T_c)/M_{\text{Co}}(0)$  and  $K_{1\text{Co}}(T/T_c)/K_{1\text{Co}}(0)$  are taken as those of  $\text{Y}_2\text{Co}_{17}$ .<sup>3</sup> The magnetic moments of the rare-earth ion and of  $R_2\text{Co}_{17}$  are given by

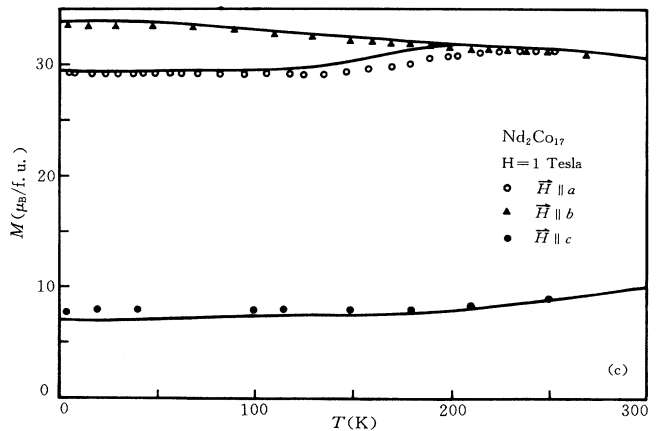
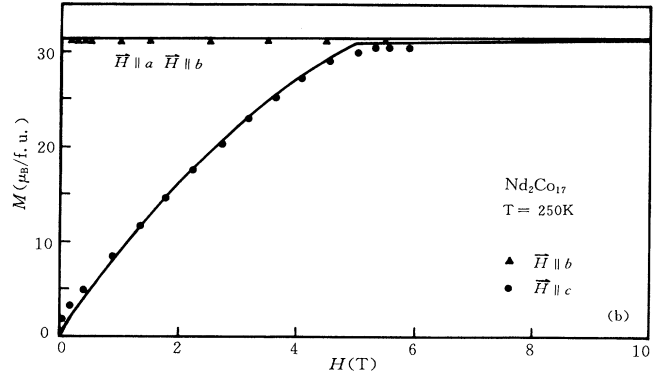
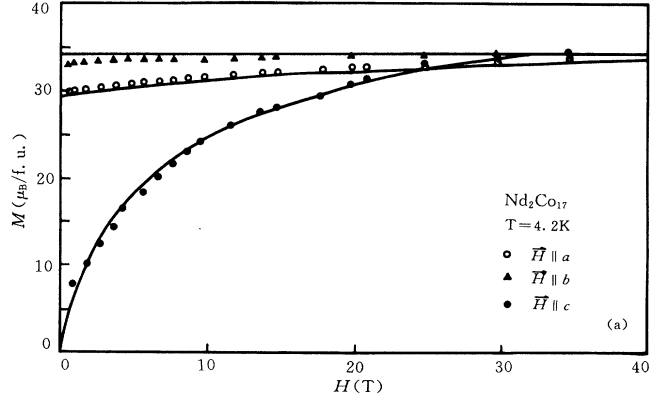


FIG. 3. Isotherms at (a) 4.2 K and (b) 250 K, and (c) the temperature dependence of magnetization in the field of 1 T for  $\text{Nd}_2\text{Co}_{17}$ . The solid lines represent the calculations. The experimental data ( $\circ$ ,  $\blacktriangle$ ,  $\bullet$ ) are from (a), (b) Ref. 4 and (c) Ref. 3.

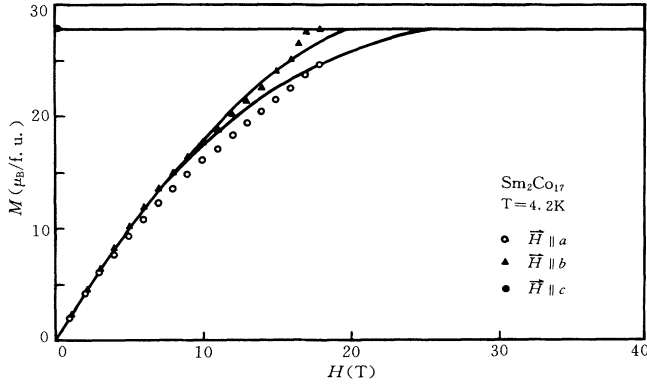


FIG. 4. Isotherms at 4.2 K for  $\text{Sm}_2\text{Co}_{17}$ . The solid lines represent the calculations. The experimental data ( $\circ$ ,  $\blacktriangle$ ,  $\bullet$ ) are from Ref. 5.

$$\mathbf{M}_R(T) = - \sum_i \mu_B \langle n_i | \mathbf{L} + 2\mathbf{S} | n_i \rangle \exp(-E_i/k_B T) / Z. \quad (7)$$

$$\mathbf{M}(T) = 2\mathbf{M}_R(T) + \mathbf{M}_{\text{Co}}(T). \quad (8)$$

The values of the parameters of  $H_{\text{ex}}$  and  $A_{nm}$  are obtained from the best fit of the calculations to the experimental data. The values of  $M_{\text{Co}}(0)$  and  $K_{1\text{Co}}(0)$  are also

adjusted around the values for  $\text{Y}_2\text{Co}_{17}$  for better fit [experimental values of  $M_{\text{Co}}(0)$ : 28.05,<sup>3</sup> 27.3,<sup>5</sup> and 28.00  $\mu_B/\text{f.u.}$  (Ref. 8) and of  $K_{1\text{Co}}(0)$ : -8.66,<sup>3</sup> -9.94,<sup>5</sup> and -6.77 K/f.u. (Ref. 8)]. The experimental data provide temperature dependence of spontaneous magnetization  $M_s(T)$ , isotherms along the crystal axes at low and high temperatures  $M(H, T = \text{const})$ , and temperature dependence of magnetization in a given field  $\mathbf{H}$  applied along the crystallographic axes  $M(T, H = \text{const})$ .

### III. RESULTS AND DISCUSSIONS

Table I lists the fitted values of  $H_{\text{ex}}(T=0 \text{ K})$ ,  $A_{nm}$ ,  $K_{1\text{Co}}(0)$ , and  $M_{\text{Co}}(0)$ . The values of the magnetic moments of the rare-earth ions  $M_R(0)$  are also listed which were calculated by using the fitted parameters. The apparently smaller than  $g_J J = 0.71 \mu_B$  value for the Sm ion is caused mainly by the mixing of the excited multiplet state of  $|J=2.5, M=-2.5\rangle$  into the ground eigenstate, i.e.,

$$|n_1\rangle = 0.982|2.5, -2.5\rangle - 0.185|3.5, -2.5\rangle + \dots$$

For  $\text{Ho}_2\text{Co}_{17}$ , the values of  $H_{\text{ex}}(T=0 \text{ K})$  and  $A_{nm}$  for the  $b$  and  $d$  site ions reported by Radwanski *et al.*<sup>11</sup> are also included for reference. The average values of  $A_{nm}$  reported by them are quite different from our results,

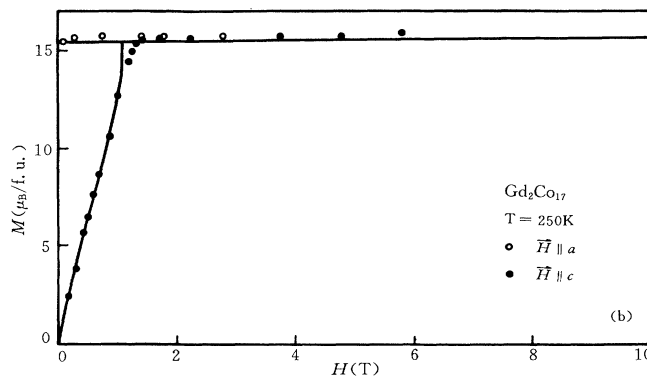
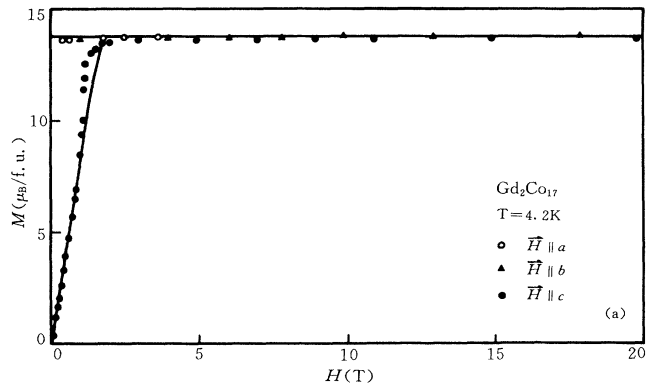


FIG. 5. Isotherms at (a) 4.2 K and (b) 250 K for  $\text{Gd}_2\text{Co}_{17}$ . The solid lines represent the calculations. The experimental data ( $\circ$ ,  $\blacktriangle$ ,  $\bullet$ ) are from (a) Ref. 6 and (b) Ref. 3.

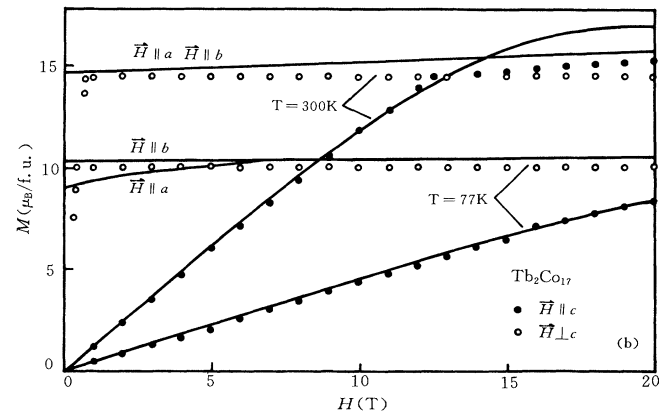
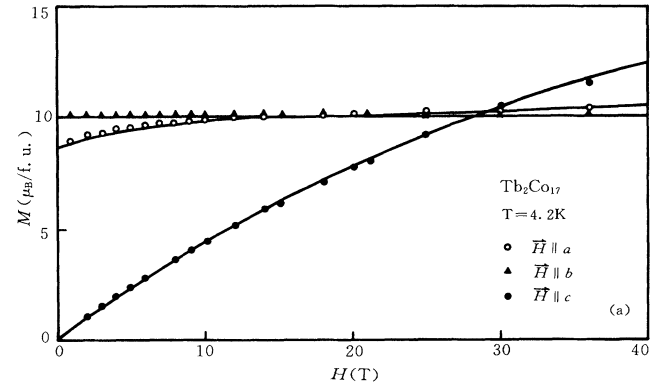


FIG. 6. Isotherms at (a) 4.2 K, (b) 77 and 300 K for  $\text{Tb}_2\text{Co}_{17}$ . The solid lines represent the calculations. The experimental data ( $\circ$ ,  $\blacktriangle$ ,  $\bullet$ ) are from (a) Ref. 3 and (b) Ref. 1.

while the value of the exchange field agrees very well.

Figures 1–9 show the comparison of the calculations with the experimental data. The solid lines represent calculations, and the circles etc., experimental data. The calculations, except  $M(H, 4.2\text{ K})$  in low fields for  $\text{Pr}_2\text{Co}_{17}$  [Fig. 2(a)], reproduce the experimental data fairly well.

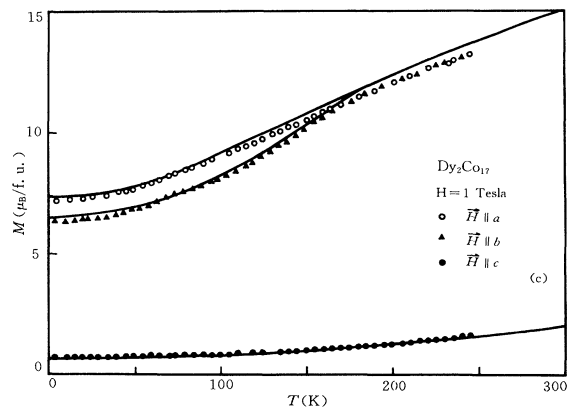
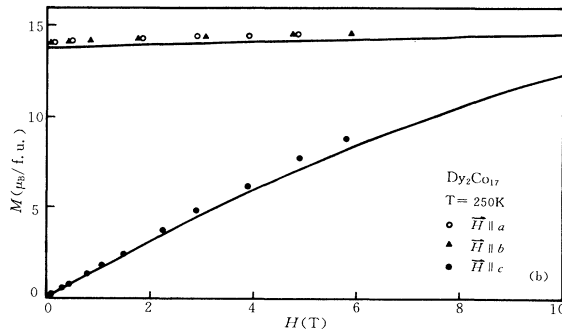
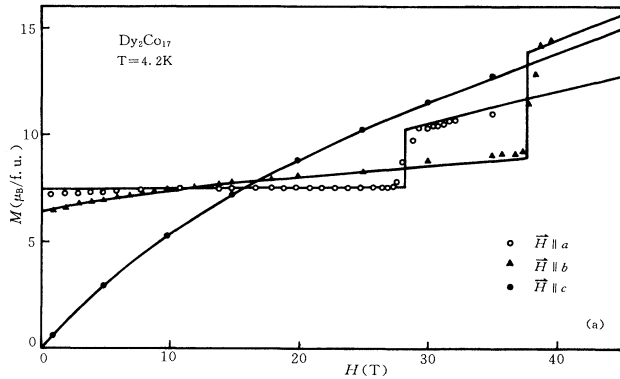


FIG. 7. Isotherms at (a) 4.2 K and (b) 250 K, and (c) the temperature dependence of magnetization in a field of 1 T for  $\text{Dy}_2\text{Co}_{17}$ . The solid lines represent the calculations. The experimental data ( $\circ$ ,  $\triangle$ ,  $\bullet$ ) are (a) from Ref. 6 and (b), (c) Ref. 3.

Figure 1(a) shows  $M_s(T)$  for the compounds of Pr, Nd, Sm, Gd, Tb, Dy, Ho, Er, and Tm. For the ferromagnetically coupled light rare-earth compounds,  $M_s(T)$  decreases monotonically with increase of temperature, while for the antiferromagnetically coupled heavy rare-earth compounds,  $M_s(T)$  increases with increase of tem-

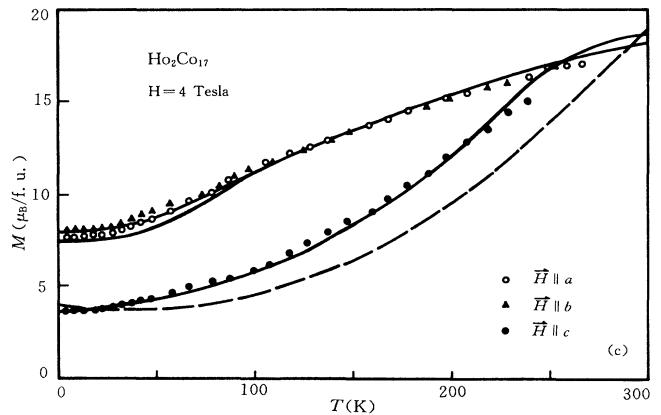
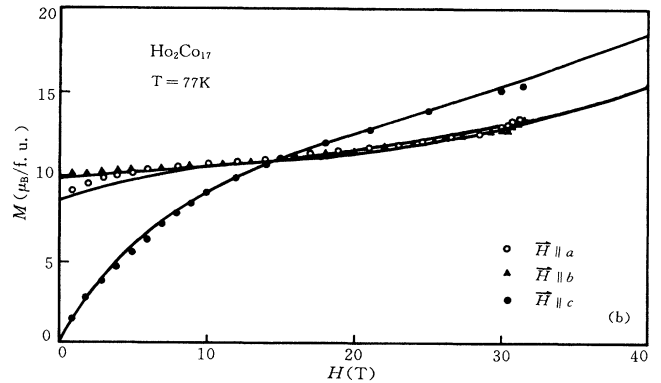
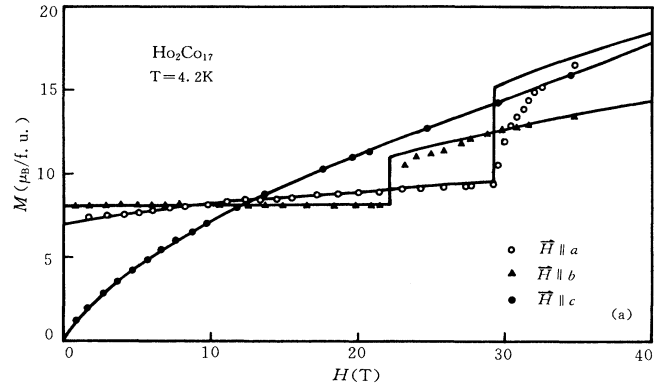


FIG. 8. Isotherms at (a) 4.2 K and (b) 77 K, and (c) the temperature dependence of magnetization in a field of 4 T for  $\text{Ho}_2\text{Co}_{17}$ . The solid lines represent the calculations. The dashed line in (c) is the calculation arrived at by using the parameters of Ref. 11. The experimental data ( $\circ$ ,  $\triangle$ ,  $\bullet$ ) are from (a) Ref. 7 and (b), (c) Ref. 3.

TABLE II.  $M(H, T)$  of  $\text{Ho}_2\text{Co}_{17}$  along the  $c$  axis and the averaged energy gap between the first excited and the ground eigenstates  $\Delta E_{0-1}$  for the two Ho ions at the  $b$  and  $d$  sites, calculated by using the different sets of  $A_{20}(b)$ ,  $A_{20}(d)$ ,  $A_{40}(b)$ , and  $A_{40}(d)$  parameters. The values of all parameters, including the average of  $A_{20}$  and  $A_{40}$ , are the same as those listed in Table I.

$A_{20}(b)$ (K)	$A_{20}(d)$ (K)	$A_{40}(b)$ (K)	$A_{40}(d)$ (K)	$M(10 T)$ ( $\mu_B/\text{f.u.}$ )	$M(20 T)$ ( $\mu_B/\text{f.u.}$ )	$M(30 T)$ ( $\mu_B/\text{f.u.}$ )	$M(40 T)$ ( $\mu_B/\text{f.u.}$ )	$\Delta E_{0-1}$ (K)
$T = 4.2 \text{ K}$								
-200	-200	-150	-150	7.22	10.84	14.04	17.82	81.54
-300	-100	-150	-150	7.22	10.82	14.02	17.80	81.48
-400	0	-150	-150	7.28	10.82	13.98	17.74	81.28
-500	100	-150	-150	7.34	10.78	13.88	17.74	80.79
-200	-200	-250	-50	7.22	10.84	14.04	17.80	81.50
-200	-200	-350	50	7.24	10.86	13.98	17.76	81.36
$A_{20}(b)$ (K)	$A_{20}(d)$ (K)	$A_{40}(b)$ (K)	$A_{40}(d)$ (K)	$M(0 \text{ K})$ ( $\mu_B/\text{f.u.}$ )	$M(100 \text{ K})$ ( $\mu_B/\text{f.u.}$ )	$M(200 \text{ K})$ ( $\mu_B/\text{f.u.}$ )	$M(300 \text{ K})$ ( $\mu_B/\text{f.u.}$ )	
$H = 4 \text{ T}$								
-200	-200	-150	-150	3.99	5.74	12.14	18.77	
-300	-100	-150	-150	4.02	5.78	12.18	18.76	
-400	0	-150	-150	4.14	5.90	12.22	18.76	
-500	100	-150	-150	4.30	6.08	12.30	18.76	
-200	-200	-250	-50	4.02	5.96	12.12	18.76	
-200	-200	-350	50	4.10	5.78	12.12	18.76	

perature since  $M_R(T)$  decreases faster than  $M_{\text{Co}}(T)$ . The small discontinuous change for the  $\text{Er}_2\text{Co}_{17}$  near 400 K is caused by the spin reorientation between the  $c$  axis and the  $c$ -plane. Figures 1(b) and 1(c) show the temperature dependences of the normalized magnetic moments  $M_R(T)/M_R(0)$  for the rare-earth ions. The experimental curves of  $M_R(T)$  have been obtained as a difference of  $M_s(T)$  of the  $R_2\text{Co}_{17}$  [Fig. 1(a)] and that of  $\text{Y}_2\text{Co}_{17}$ .<sup>2</sup> The calculation shows that  $\mathbf{M}_{\text{Sm}}$  becomes antiparallel to  $\mathbf{M}_{\text{Co}}$  above 330 K, while the experimental curve shows no such change [Fig. 1(b)]. The experimental result is doubtful because  $M_{\text{Sm}}(0) = 0.4\mu_B$  is only 1.4% of  $M_s(0) = 27.8\mu_B$ , so the experimental error for it should be very large. It can be easily seen by comparison of the  $M_s(T)$  curves of  $\text{Sm}_2\text{Co}_{17}$  and  $\text{Y}_2\text{Co}_{17}$ ,<sup>2</sup> that a slight increase of  $M_{\text{Co}}(T)$  results in the reverse of  $\mathbf{M}_{\text{Sm}}$  direction at higher temperatures. Figures 2(a) and 2(b) are  $M(H, 4.2 \text{ K})$  and  $M(H, 250 \text{ K})$ , respectively, for  $\text{Pr}_2\text{Co}_{17}$ . The spin-reorientation temperature was calculated to be 87 K in contrast to  $> 200 \text{ K}$  reported in Ref. 4. Figures 3(a), 3(b), and 3(c) are  $M(H, 4.2 \text{ K})$ ,  $M(H, 250 \text{ K})$ , and  $M(T, 1 T)$ , respectively, for  $\text{Nd}_2\text{Co}_{17}$ . A remanence is observed for the experimental  $M(H, 4.2 \text{ K})$  curves along the  $c$  axis, implying that the field has been applied along the direction of the  $c$  axis, but misoriented by a small angle. The calculation, meanwhile, was carried out along the  $c$  axis. Figures 4, 5(a), 5(b), 6(a), and 6(b), are  $M(H, 4.2 \text{ K})$  for  $\text{Sm}_2\text{Co}_{17}$ ,  $M(H, 4.2 \text{ K})$  and  $M(H, 250 \text{ K})$  for  $\text{Gd}_2\text{Co}_{17}$ , and  $M(H, 4.2 \text{ K})$ ,  $M(H, 77 \text{ K})$ , and  $M(H, 300 \text{ K})$  for  $\text{Tb}_2\text{Co}_{17}$ , respectively. Figures 7(a), 7(b), and 7(c) shows  $M(H, 4.2 \text{ K})$ ,  $M(H, 250 \text{ K})$ , and  $M(T, 1 T)$ , respectively, for  $\text{Dy}_2\text{Co}_{17}$ . Figures 8(a), 8(b), and 8(c) are  $M(H, 4.2 \text{ K})$ ,  $M(H, 77 \text{ K})$ , and  $M(T, 4 T)$ , respectively, for  $\text{Ho}_2\text{Co}_{17}$ . The calculated energy gap between the first excited and the ground eigenstates at 4.2 K is 81.5 K in good agreement with the experimental value of 82.4 K.<sup>14</sup> The calcu-

lations arrived at by using the parameters reported by Radwanski *et al.*<sup>11</sup> are also compared with the experimental data. Although they simulate the isotherms and the energy gap at 4.2 K well, they fail to reproduce the isotherms along the  $c$  axis at high temperatures as shown by the dashed line in Fig. 8(c). At this point, it would be worthwhile to show that the magnetization curves and the averaged energy gap for the two rare-earth ions at the  $b$  and  $d$  sites in the heavy rare-earth compounds, which are calculated by taking into account the difference of the two rare-earth ion sites, are the same as those calculated by neglecting the difference and using the CEF parameters averaged over the two-ion sites, if the difference of  $A_{nm}$  at the two sites is not very large. Table II demonstrates these circumstances for  $\text{Ho}_2\text{Co}_{17}$ . The first-order moment reorientations observed in Figs. 7(a) and 8(a) are of the "exchange-related" type, the physical picture of which has been described in Ref. 6. Figures 9(a), 9(b), and 9(c) are  $M(H, 4.2 \text{ K})$ ,  $M(H, 200 \text{ K})$ , and  $M(T, 4 T)$ , respectively, for  $\text{Er}_2\text{Co}_{17}$ .

From Table I, it can be seen that  $H_{\text{ex}}(0)$  decreases monotonically across the rare-earth series from Pr to Er.  $A_{20}$  varies between  $-200$  and  $-260$  except that it is  $-80 \text{ K}$  for the Pr ion. A similar but more striking anomaly has been obtained for the Pr ion in  $R\text{Co}_5$  compounds.<sup>15</sup> The anomalies would be closely related to the anomalous smaller cell volumes of both  $\text{Pr}_2\text{Co}_{17}$  and  $\text{PrCo}_5$ , compared with those extrapolated from the heavier rare-earth compounds.<sup>16,17</sup> It has been shown that both the magnetic moment and the hyperfine field of the Pr ion in  $\text{PrCo}_5$ , measured in experiments are much smaller than those calculated by using the fitted CEF parameters. This is in contrast to the good agreement observed for Sm and Dy ions in  $\text{SmCo}_5$  and  $\text{DyCo}_5$ , and it has been suggested that the Pr ion is valence fluctuated.<sup>18</sup> It would be reasonable to assume that the Pr ion in

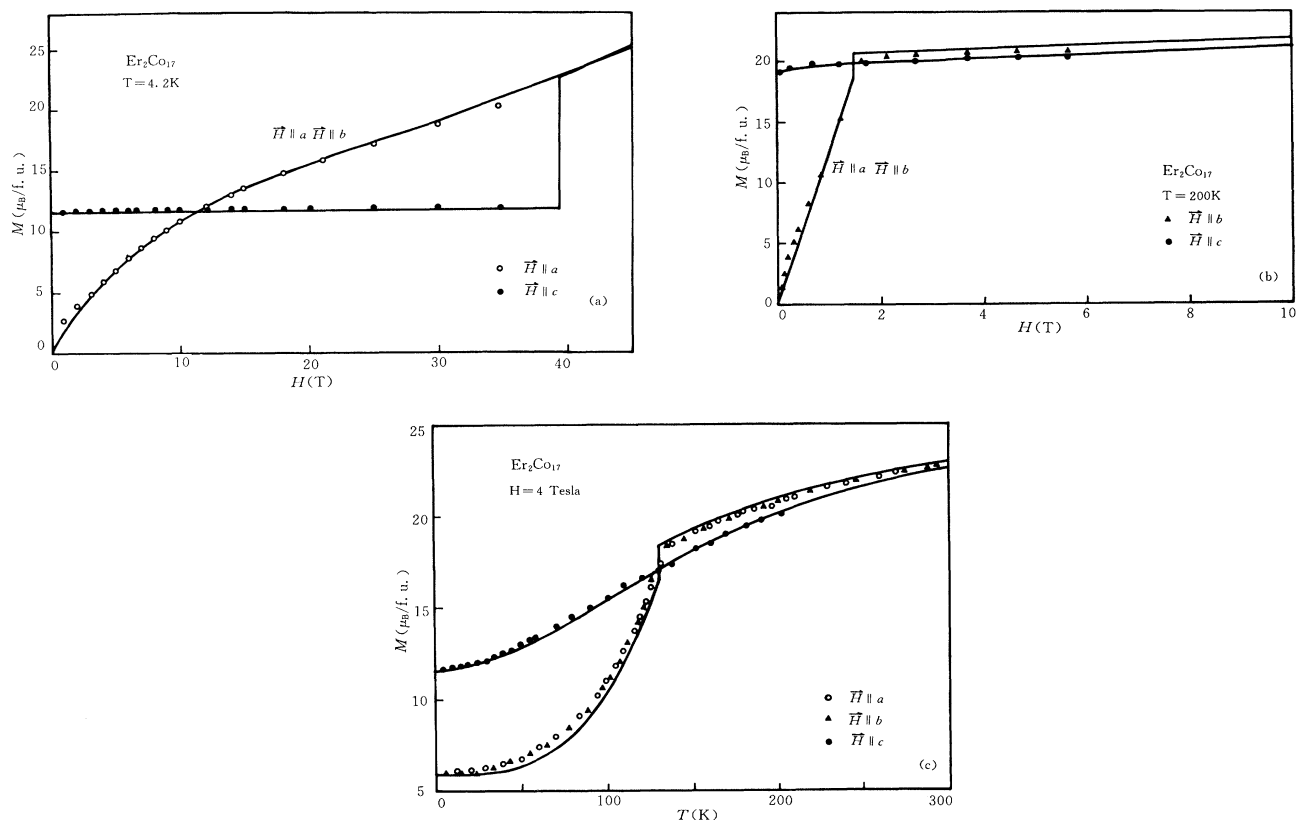


FIG. 9. Isotherms at (a) 4.2 K and (b) 200 K, and (c) the temperature dependence of magnetization in a field of 4 T for  $\text{Er}_2\text{Co}_{17}$ . The solid lines represent the calculations. The experimental data ( $\circ$ ,  $\blacktriangle$ ,  $\bullet$ ) are from (a)–(c) Ref. 3.

$\text{Pr}_2\text{Co}_{17}$  is also valence fluctuated. The failure of the calculations in simulating the spin-reorientation temperature and the  $M(H, 4.2 \text{ K})$  curves in low fields for  $\text{Pr}_2\text{Co}_{17}$  [Fig. 2(a)] would be caused by the inappropriate assumption that the Pr ion is triply ionized.

#### ACKNOWLEDGMENT

This work was supported by the Magnetism Laboratory, Institute of Physics, Chinese Academy of Sciences, Beijing, China.

- <sup>1</sup>A. V. Deryagin and N. V. Kudrevatykh, *Phys. Status Solidi A* **30**, K129 (1975).
- <sup>2</sup>N. V. Kudrevatykh, A. V. Deryagin, A. A. Kazakov, V. A. Reymer, and V. N. Moskalev, *Fiz. Met. Metalloved. (USSR)* **45**, 1169 (1978).
- <sup>3</sup>S. Sinnema, thesis, Natuurkundig Laboratorium der Universiteit van Amsterdam, The Netherlands, 1988 (unpublished).
- <sup>4</sup>R. Verhoef, J. J. M. Franse, F. R. de Boer, H. J. M. Heeroms, B. Matthaai, and S. Sinnema, *IEEE Trans. Magn.* **24**, 1948 (1988).
- <sup>5</sup>A. V. Deryagin, N. V. Kudrevatykh, and V. N. Moskalev, *Phys. Met. Metallogr. (USSR)* **54**, 49 (1982).
- <sup>6</sup>J. J. M. Franse, R. J. Radwanski, and R. Verhoef, *J. Magn. Magn. Mater.* **84**, 299 (1990).
- <sup>7</sup>S. Sinnema, J. J. M. Franse, R. J. Radwanski, A. Menovsky, and F. R. de Boer, *J. Phys. F* **17**, 233 (1987).
- <sup>8</sup>B. Matthaai, J. J. M. Franse, S. Sinnema, and R. J. Radwanski, *J. Phys. (Paris) Colloq.* **49**, C8-533 (1988).
- <sup>9</sup>R. J. Radwanski, J. J. M. Franse, and S. Sinnema, *J. Magn. Magn. Mater.* **51**, 175 (1985).
- <sup>10</sup>R. J. Radwanski, J. J. M. Franse, S. Sinnema, H. J. M. Heeroms, and J. H. P. Colpa, *J. Magn. Magn. Mater.* **76**, 182 (1988).
- <sup>11</sup>R. J. Radwanski and J. J. M. Franse, *Physica B* **154**, 181 (1989).
- <sup>12</sup>B. G. Wybourne, *Spectroscopic Properties of Rare Earths* (Interscience, New York, 1965).
- <sup>13</sup>S. Hufner, *Optical Spectra of Transparent Rare-Earth Compounds* (Academic, London, 1978), p. 34.
- <sup>14</sup>K. Clausen and B. Lebech, *J. Phys. C* **15**, 5095 (1982).
- <sup>15</sup>Zhao Tie-song, Jin Han-min, Guo Guang-hua, Han Xiu-feng, and Chen Hong, *Phys. Rev. B* **43**, 8593 (1991).
- <sup>16</sup>W. Ostertag and K. J. Strnat, *Acta Crystallogr.* **21**, 560 (1966).
- <sup>17</sup>H. Wernick and S. Geller, *Acta Crystallogr.* **12**, 662 (1959).
- <sup>18</sup>Jin Han-min, Kenji Shimizu, Han Xiu-feng, Yan Yu, and Zhao Tie-song, *J. Phys. Condens. Matter* **4**, 8609 (1992).